Lasers in Surgery and Medicine 19:249–259 (1996)

Stress-Wave-Induced Injury to Retinal Pigment Epithelium Cells In Vitro

Tina Douki, MS, Shun Lee, PhD, Kathleen Dorey, PhD, Thomas J. Flotte, MD, Thomas F. Deutsch, PhD, and Apostolos G. Doukas, PhD

Wellman Laboratories of Photomedicine, Massachusetts General Hospital and Harvard Medical School (T.D., S.L., T.J.F., T.F.D., A.G.D.) and Schepens Eye Research Institute and Harvard Medical School, Boston, Massachusetts 02114 (K.D.)

Background and Objective: **To determine the survival of in vitro retinal pigment epithelium (RPE) cells subjected to laser-generated stress transients (shock waves) and compare it to that of other cell lines.**
Study Design/Materials and Methods: **Normal and transformed human retinal pigment epithelium cell lines were used. The cells were imbedded in a gel to prevent motion and cavitation and located in a thin layer at the bottom of a pipette tube closed at one end by a polyimide film. Stress transients were generated by pulsed excimer laser (193 nm and 248 nm wavelength) ablation of the polyimide film. Cell survival, compared to that of unirradiated cells, was assessed by counting surviving cells. The stress was varied from 300 to 740 bars and the number of shock wave pulses applied varied from 5 to 150.**
Results: **Cell survival decreased sharply at the higher stresses but some cells always survived. The lowest survival rate was 50%. Increasing the number of shock wave pulses did not increase cell killing after 20 pulses, demonstrating a saturation effect. In contrast to the transformed cell line, normal cells could not be killed at the highest stress available to us.**
Conclusion: **The susceptibility of RPE cells to damage by stress waves varies with cell line. Transformed retinal pigment epithelium cells are more susceptible than normal ones. Saturation of the damage versus number of pulses is observed and a threshold-like behavior for cell killing versus stress is found. Because at least 50% of the cells survived, normal cell growth can serve to replenish damaged cells.**

Key words: shock waves, stress transient, cell killing, retinal pigment epithelium

INTRODUCTION

The role of mechanical effects in laser-tissue interactions was recognized soon after the use of the laser in medicine [1], but their study was hindered by the fact that these effects were usually only one of several processes initiated by the laser. Early studies of the interaction of the pulsed ruby laser with the retina noted that both mechanical and thermal components are present in the lesions produced and further differentiated mechanical effects due to the passage of a high pressure front from those due to localized bulk displacement [2,3]. Today it is recognized that laser-induced mechanical effects can be therapeutically useful, as in laser lithotripsy for kidney stone fragmentation [4–7], pulsed laser vasodilation for cerebral vasospasm [8], or laser-based phacoemulsification [9]. Laser-induced mechanical effects can have deleterious ancillary consequences accompanying laser-tissue interactions, as in the case of cavitation accompanying oph-

Accepted for publication November 3, 1995.

Address reprint requests to Thomas F. Deutsch, Ph.D., WEL 224, Massachusetts General Hospital, 55 Fruit Street, Boston, MA 02114.

thalmic photodisruption [10], or bubble formation accompanying laser angioplasty [11].

The growing use of short pulse lasers in ophthalmology, as well as in other fields of medicine, has led to increased interest in their mechanical effects. A number of studies have shown that ns and ps laser-induced optical breakdown, clinically referred to as ophthalmic photodisruption, induces plasma formation, cavity growth and collapse, and pressure waves propagating at supersonic velocities [12–15]. Pulsed laser ablation of tissue and polymer films serving as tissue models has been shown to launch pressure waves which can lead to tissue damage [16,17]. However, studies of the biological effects of pressure transients have been hindered by the difficulty of generating well-characterized pressure pulses whose temporal and spatial characteristic are known.

Recently the pressure pulses generated by excimer laser ablation of polyimide films have been characterized and mathematically modeled [18]. Pulses with peak pressures as high as 10 kbar and rise times shorter than 10 ns were generated. The laser ablation of a polymer, such as polyimide, provides a simple laboratory system of generating repetitive pressure pulses for biological experimentation. As discussed in more detail below, with proper care this system can avoid a number of confounding effects, such as cavitation, significant transient heating and photodissociation, among others.

Cellular and tissue response to stress waves has been the subject of a number of recent papers [16,19–22]. Many of these experiments used lithotripters designed for urology as a source of shock waves. These experiments have established that shock waves can be used to permeabilize the plasma membrane of cells [23–25] and have demonstrated the ability of shock waves to enhance the toxicity of drugs such as cisplatin and doxorubicin in cells [26–29]. More generally, these experiments have shown that shockwaves have the potential to permeabilize cells for the delivery of a wider variety of drugs. However the lithotripter, in addition to producing shock waves, may produce tissue and cellular effects by a variety of other mechanisms, such as cavitation and free radical formation. In addition, the shock wave risetime, which can be significant for killing of some cells [16], depends on the type of lithotripter and may range from < 30 ns to over 600 ns [7].

Our group has focused on the use of controlled, laser-generated stress waves in a system free of confounding ancillary effects, such as cavitation, free radical formation or transient heating, to study cellular effects. Cell damage was assayed using both morphological (transmission electron microscopy) and functional (incorporation of tritiated thymidine) assays, with the latter being the more sensitive assay [20]. In these studies, which used a mouse breast sarcoma cell line (EMT-6), we found that cellular damage by stress waves correlates better with the rate of rise of the stress wave than with its peak value. We interpreted that result in terms of the similarity between the spatial extent of the stress gradient and typical cellular dimensions. Since the stress wave generated in our experiments propagates at or slightly above the speed of sound, the rise time corresponds to the spatial gradient of the stress across the cell. For a sound velocity of 1500 m/s a pressure pulse rise time of 10 ns, typical of these experiments, corresponds to a spatial gradient of stress extending over 15 μm, a dimension comparable to that of many cells. We also found that uptake of tritiated thymidine, a measure of cell viability, decreased approximately linearly with stress gradient; no evidence of any threshold for cell killing was found. While the mechanism of cellular damage by stress transients has not been unambiguously established, the transient generation of pores in the cell membrane may be involved. Observations consistent with this possibility include the stress wave induced enhancement of drug cytotoxicity [1], as well as initial direct observations of the transport of fluorescent dyes through the cell membrane after exposure to a stress transient. The latter studies demonstrated that stress-wave-induced permeability of EMT-6 cells persists for many seconds [25].

The objective of this study was to investigate stress wave damage to retinal pigment epithelium (RPE) cells in culture in order to determine their damage thresholds and the parameters governing stress wave damage. As only the EMT-6 cell line has been studied to date, this study allows the generality or specificity of those results to be compared to those in a different cell line. Since we studied both normal and transformed RPE cells, we could determine the effect transformations of a single cell line on susceptibility to stress waves.

This study is part of a larger program investigating ocular damage of all types caused by ultrashort pulses. In addition, with the increasing use of short pulses in clinical ophthalmology, the results obtained here may be relevant to the ancillary effects of ophthalmic laser ablation proce-

dures, such as cutting of vitreous bands near the retina. It should be noted, however, that in actual clinical procedures the source of mechanical injury may be more complex than in this idealized system. For example, cutting of vitreous bands might injure the retina both via shock waves launched from an expanding cavity or bubble and via jets formed when such a cavity touches a boundary, the retina [15,30]. Furthermore, the injury may be gross and at the tissue, rather than the cellular level studied here. Another example of potential ophthalmic interest is laser refractive surgery, in which ablation is known to induce a shock wave which may propagate and injure the corneal endothelium. Stress wave induced transient increases in membrane permeability have been proposed as a means for delivering drugs [1,26]; hence an understanding of how much such effects depend on cell line will help in assessing the generality of the approach.

MATERIAL AND METHODS

Experimental System

Figure 1 shows the experimental arrangement for irradiation, as well as a flow diagram of the experiments. This experimental arrangement has been discussed in previous publications [20] and is discussed in detail below.

Stress Wave Generation

Stress waves were generated using excimer laser ablation of polyimide films which formed one end of a pipette tube containing the target cells. The excimer laser (Lambda Physik, model EMG 103MSC, Acton, MA) operating at a pulse repetition rate of 1 Hz was used at two wavelengths, 193 nm from argon-fluoride [ArF] and 248 nm from krypton-fluoride [KrF]. The 1 Hz repetition rate was chosen to minimize heating effects while maintaining reasonable irradiation times. These two laser wavelengths were used because they resulted in the generation of stress waves with different rise times and stress rise time has been shown to be a significant variable in determining cellular damage in EMT-6 cells [16]. The rectangular laser beam was focused to a rectangular spot 6 × 3 mm in size on the polyimide film closing the 1.5 mm nominal inner diameter pipette tubes. Pipette tubes, rather than larger cell containers, were used in order to obtain as high a laser fluence, and hence stress, as possible for the laser energy available. The pulse energy was varied from 25 to 240 mJ using quartz attenuators in order to vary the peak stress.

Ablation of the polyimide generates reaction forces which launch a stress wave in the polyimide. A key feature of these experiments is the use of a laser system for generating stress waves without undesired ancillary effects, such as heating, cavitation, or photochemical reactions. As discussed in detail by Zweig et al. [18], the strength of stress wave depends upon the fluence incident on the polyimide. In order to determine the amplitude and rise time of the stress pulse, measurements of the stress wave induced by a given laser fluence were made before each experiment. This was done using a calibrated PVDF (polyvinyledene fluoride) transducer as described by Zweig et al. [1,8]. A 75-μm polyimide film, identical in thickness to that used to seal the pipette, was placed on the transducer using silicon grease for acoustic contact. An aperture was positioned over the central part of the laser beam with the transducer mounted directly behind it. The transducer signal was recorded by a storage oscilloscope (Tektronix 7934, Tektronix Inc., Beaverton, OR) or a programmable digitizer (Tektronix 7912AD) using a 1 MΩ termination. The temporal resolution of the transducer-oscilloscope system was measured to be 5 nsec.

The pressure applied to cell cultures differs from the pressure measured by the transducer because the acoustic impedances of polyimide, Z_1, (3.1 MPa m^{-1} s) and gel, Z_2, (1.6 MPa m^{-1} s) are different. From the values of the acoustic impedances the correction factor for the plane wave geometry applicable here can be calculated using the expression $2Z_1/(Z_1 + Z_2)$. The pressure in the gel is about 32% higher than that in the polyimide. The values of pressure presented here are the corrected values of pressure in the gel.

A number of potential artifacts were considered and eliminated in order to assure that the effects observed were due to the laser-generated stress waves. Ultraviolet radiation from the laser sources is prevented from striking the cells by the strong absorption of the polyimide film, which has an optical absorption length of less than 1 μm at the 193 and 248 nm laser wavelength(s). In addition, the absorption of polyimide film prevents any light with wavelengths shorter than 500 nm generated by ablation from reaching the gel. The steady state heating by absorbed laser energy is limited by the low average power of the laser, less than 0.25 W, and has been measured to be less than 1°C in the cells for 150 pulses at 1 Hz. Cav-

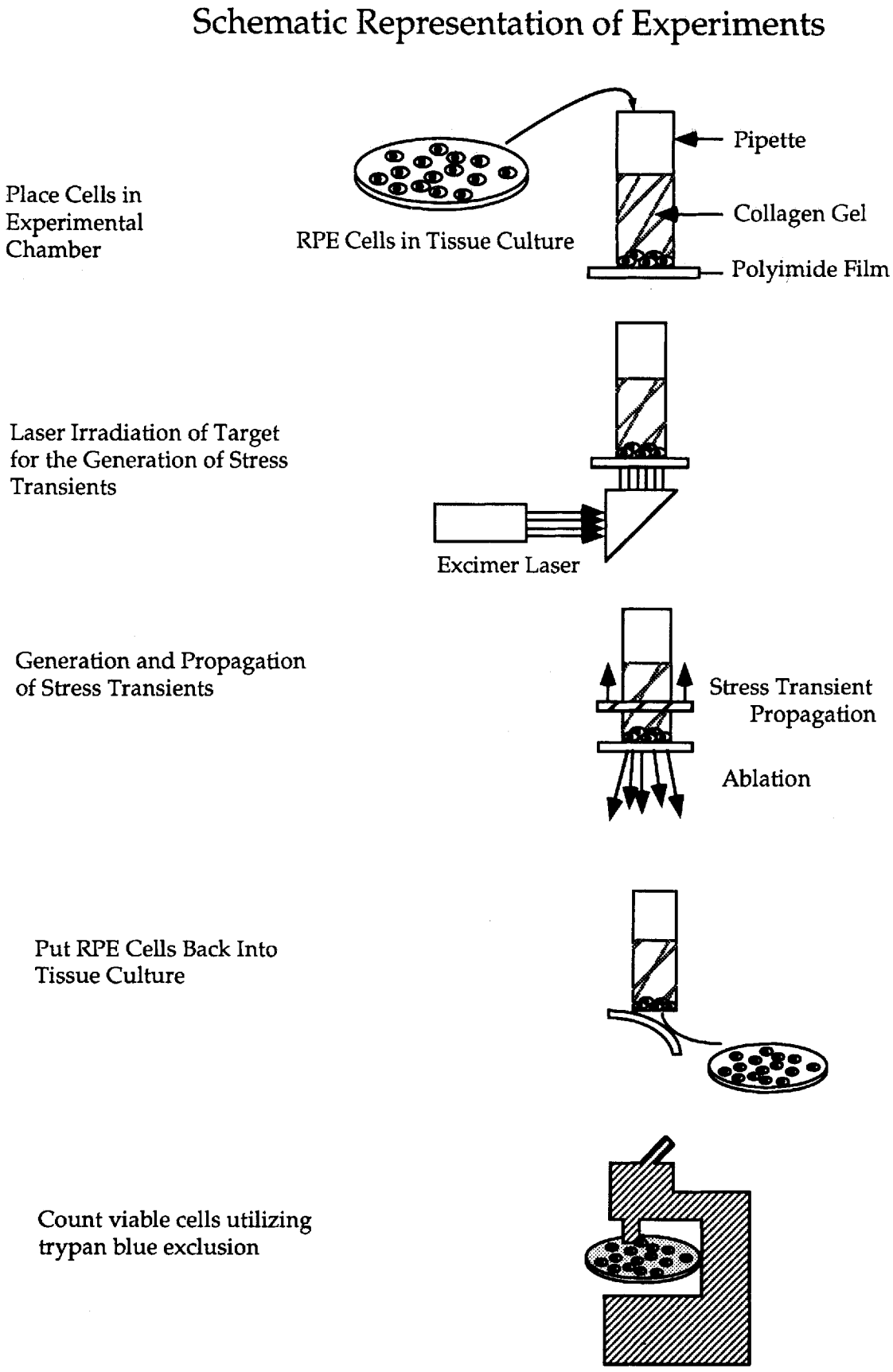

Fig. 1. Schematic diagram of the experimental procedure and apparatus. Note that the cells occupy only a thin (200 μm) layer at the bottom of the pipette tube.

itation was minimized and possibly eliminated by immobilizing the cells in a collagen gel [31]. Cavitation is known to result in free radical formation. In previous experiments Fricke dosimetry, a colorimetric test for the presence of free radicals, was applied and no free radicals detected within the limit of the measurement [32]. The possibility that the entire polyimide membrane might undergo deformation which could lead to cell injury was investigated by using a He-Ne laser beam parallel and in close proximity to the polyimide surface to probe its deflection as the polyimide was irradiated. A silicon photodiode showed no change in He-Ne laser intensity during irradiation, indicating that the deformation of the polyimide was much less than the 25 μm resolution of the system.

The rise time of a stress wave can change as it propagates in a medium, shortening due to pressure-dependent acoustic propagation velocities or lengthening due to frequency-dependent acoustic attenuation. In our experiments, however, these phenomena are negligible because of the thin samples (< 200 μm) employed. We used the pressure transducer described below to measure the rise time of the stress pulse and determine that propagation through 150 μm of gel, typical of the thickness of the cell layer, did not change the rise time. It should be noted, however, that propagation over sufficiently long distances can change the rise time; in separate experiments to study the propagation of stress waves in the vitreous of bovine eyes we found that the stress wave rise time decreased by over a factor of two in propagating through 1 mm of vitreous.

Figure 2 shows the pressure versus time for the stress waves generated during the ablation of polyimide by ArF and KrF lasers. Although both stress waves have approximately the same duration, their rise times differ substantially. ArF ablation of polyimide generates a stress wave with a rise time of ~10 nsec, while KrF ablation generates a stress wave with a rise time of ~20 nsec. The rise times of the stress waves remained constant over the range of stress amplitudes employed in the experiments. The difference in stress rise time for laser pulses having similar (20 ns) pulse widths arises from the different absorption lengths of the laser radiation in polyimide at the two wavelengths [18].

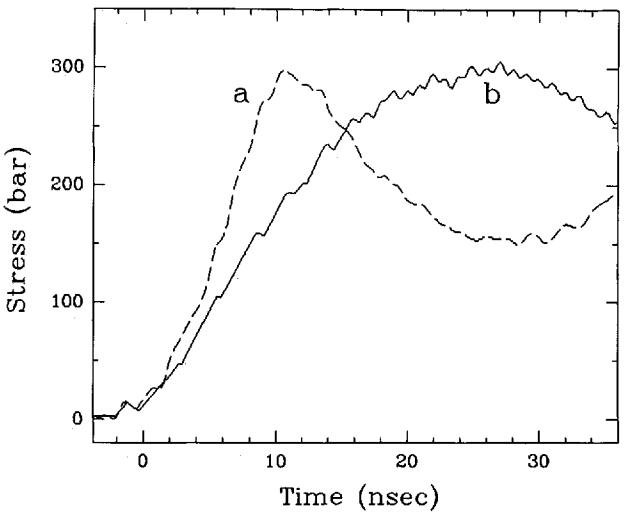

Fig. 2. Signal from a PVDF transducer detecting stress waves generated by the ablation of a polyimide film by ArF (a) and KrF (b) laser radiation. The pressure is obtained using a transducer calibration constant of 2 mV/N. The beam diameter was 2.3 mm, and the temporal resolution of the transducer-oscilloscope system was ~5 ns.

Target Cells

Two types of RPE cells were used as targets, normal cells established from donors over age 70, and an immortalized cell line RPE 28 SV, obtained by transformation of a fetus-derived retinal pigmented epithelial cell (Depository #AG06096A, Coriell Cell Repositories, Camden, NJ). The homogeneity of these normal cell lines was demonstrated by the regularity of the polygonal epithelial cells and their ability to form melanin. When tested for cytokeratin intermediate filaments (a marker for epithelial cells), every cell in the culture exhibited bright perinuclear staining; the control cells stained without the primary antibody were negative. Cytokeratin immunohistochemistry was performed with mouse monoclonal Anti-Pan cytokeratins (against peptides 1,4,5,6,8,10,13,18,19; Sigma Chemical Co., St. Louis, MO) and a streptavidin-alkaline phosphatase kit (Kirkegaard & Perry, Gaithersburg, MD). The culture media was changed at weekly intervals until they were nearly confluent (approximately 80% area coverage). Confluence was avoided to eliminate any possible effects of contact inhibition on cell cycle distribution and length. The cells were trypsinized (Trypsin-0.25% EDTA, GIBCO, Grand Island, NY), washed, and centrifuged once in complete medium and twice in Dulbecco's Phosphate Buffered without calcium or magnesium (PBS-Fisher Scientific, Pittsburgh, PA).

The medium used for the immortalized cell line was Dulbecco's Modified Eagles Medium

(DMEM) with phenol red, enriched with 10% fetal bovine serum (FBS) and 1% sodium pyruvate (GIBCO, Grand Island, NY); DMEM with phenol red, enriched with 5% FBS and 2% low protein serum replacements LPSR-1 (Sigma, St Louis, MO) was used for the normal line.

The normal line cells underwent from 3 to 6 passages before being used in an experiment; the number of passages was limited to less than 7 to maintain similarity to the parent cells. The transformed cells were maintained for a period of about 1.5 years; some were stored in liquid nitrogen until needed and some were grown immediately, undergoing three passages per week. The transformed cells underwent between 45 and 80 passages before being used in an experiment; unlike the normal cells the transformed cells can be passed many times and still retain their similarity to the starting cells. Hence for these cells the number of passages was simply determined by when the cells were needed for an experiment.

The cells were adjusted to a concentration of 3×10^6/ml in PBS containing 5% Knox gel (denatured collagen) at 37°C. Subsequently, 50 μl of the cell suspension was placed in a 200 μl micropipette with a nominal inner diameter of 1.5 mm (VWR Scientific, Westwood, MA) sealed at one end with 75 μm thick polyimide (300 HN Kapton, DuPont, Wilmington, DE), resulting in a gel column approximately 2.7 cm tall containing 1.5×10^5 cells. The seal at the end of the pipette was water tight to prevent any water seepage into the gels. Each pipette was then placed in a 5 ml test tube filled with water and was kept in a water bath at 37°C. The test tubes were then centrifuged at 1200 RPM for 10 minutes in order to bring the cells to the polyimide at the end of the pipette. The cells then formed a thin layer in contact with the polyimide. The thickness of this layer is estimated to be 100 μm by noting there are 1.5×10^5 cells with a radius of 5 μm in our 1.5 mm (nominal) i.d. pipettes. We used light and electron microscopy to show that this procedure resulted in a cell layer about 200 μm thick. Hence, our irradiation geometry was a planar layer of cells whose diameter/height ratio was greater than 7. As discussed above, the upper limit on the thickness of the planar layer of cells was determined by the need to avoid alteration of the stress wave with propagation while the lower limited was determined by the need to have an adequate number of cell to analyze. Finally the pipette tubes were placed in an ice water bath to complete the solidification of the gel and to slow down the metabolism of the cells.

Irradiation and Analysis

The cells were exposed to 5–150 laser-generated stress transients having different stress values. After exposure to stress waves at room temperature, the pipette tubes were warmed to 37°C to melt the gel. The polyimide was then removed gently and the contents of each pipette tube flushed with 0.5 ml PBS into separate 5-ml test tubes. These test tubes were spun at 1200 RPM for 10 minutes. After centrifugation the supernatant in each tube was aspirated and discarded. The cell pellets were then resuspended in 300 μl of complete medium enriched with 1% antibiotics (200 units/ml of penicillin and 200 units/ml of streptomycin) and plated in a 24-well flat-bottom culture plate. In addition, we used as controls pipette tubes with cells which were subjected to the same procedure as above, but which were not exposed to laser-generated stress transients.

In order to determine if there were both acute and delayed effects of irradiation, cell survival was determined immediately after irradiation, as well as at times as long as 12 hours after irradiation. The plates containing the immortalized cell line were incubated for 4, 8, or 12 hours while the normal cells were incubated for 24, 48, and 72 hours. The number of surviving cells were counted using a Trypan blue exclusion assay. In preliminary experiments, it was shown that trypan blue exclusion compares well with clonogenic assays and thymidine incorporation. The surviving cell population was expressed as a percentage of the number surviving in control pipettes not exposed to stress waves. At least ten different and independent measurements of the viability, involving at least 5 pipettes each, were taken for each experimental set of conditions and averaged to obtain each point on the cell survival curves. Thus, each data point represents the results of measurements on at least 50 irradiated pipettes and 50 control pipettes, each containing of the order of 10^5 cells.

Cells were also examined by transmission electron microscopy. After irradiation, the polyimide was removed from the pipettes under a dissecting microscope and the gel samples were gently extruded into vials containing 4% gluteraldehyde fixative. After initial overnight fixation, the gels were rinsed in 0.1 M cacodylate buffer and post-fixed in 2% OsO_4 for 2 hours. The samples were then dehydrated in a graded ethanol

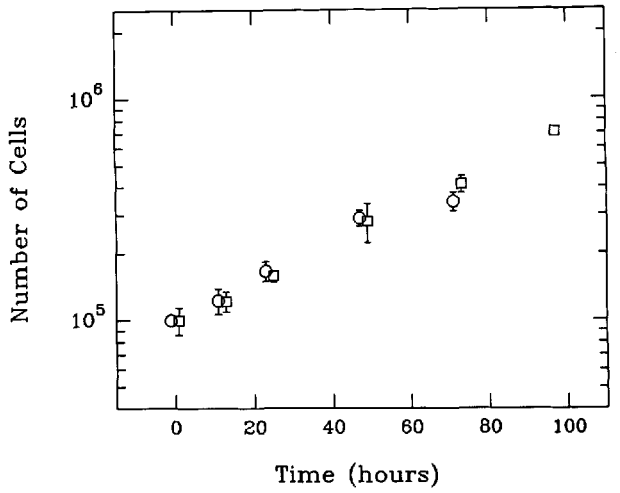

Fig. 3. Number of cells vs. time for immortalized (transformed) RPE cells free on cell dishes (*open circles*) and in pipettes (*open triangles*). The growth rate of the cells is unaffected by confinement in the pipettes.

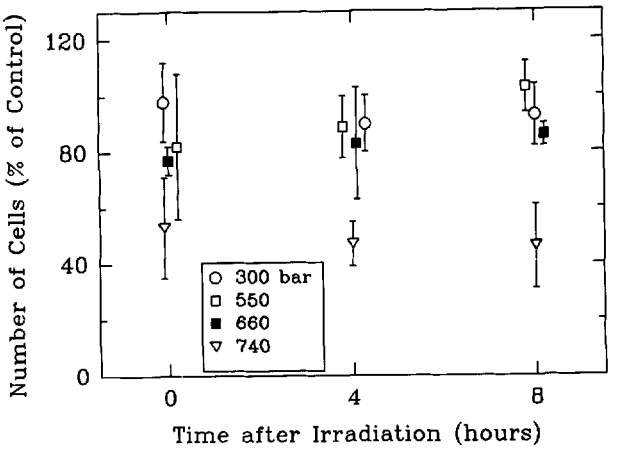

Fig. 4. Number of surviving cells, expressed as percent of unirradiated control cells, vs. number of hours of incubation between irradiation and analysis, for four different peak pressures and 20 pulses. Each data point represents measurements on at least 50 pipette tubes, each containing of the order of 10^5 cells. The error bars represent standard deviations.

series and flat embedded with Epon 812 (Electron Microscopy Sciences, Fort Washington, PA). One-micron-thick cross-sections were cut through the samples for light microscopy on an ultramicrotome (Reichert-Jung Ultracut, Vienna, Austria) and stained with 1% toluidine blue. Ultrathin sections were cut, stained with uranyl acetate and lead citrate, and then examined with a transmission electron microscope (CM-10, Philips, Eindhoven, The Netherlands).

RESULTS

Figure 3 shows the results of a control experiment that examined the effect of the pipette environment on cell growth. The growth curves for transformed cell line are essentially identical for free cells and cells in pipettes, indicating that confinement in the pipettes did not alter the doubling time of the cells significantly.

Figure 4 shows survival of transformed cells, expressed as percent of control, vs. time after irradiation for four different values of peak pressure. For a given pressure there is no statistically significant change in the survival of cells for assay times of 0, 4, and 8 hours after irradiation. These data were normalized to the number of unirradiated control cells surviving at the same time in order to correct for the effect of normal cell growth. This indicates that there are no chronic or delayed effects of irradiation. The data do indicate a clear and statistically significant decrease in survival at the highest stress, 740 bars.

Figure 5 shows survival of transformed RPE cells vs. peak stress for 20 pulses at 4 hours after irradiation and illustrates the threshold like behavior of the survival curve. The curve combines data obtained using both the 193 nm ArF and the 248 nm KrF lasers, which produce stress waves having different rise times, 10 and 20 ns respectively. At stresses of 550 bars or less only a small (10%) cell killing effect is found; above this stress the cell killing effect increases rapidly with increasing peak stress reaching a maximum of 50%. Limitations in the peak stress and stress rate we could obtain with the available laser pulse energy prevented us from exploring this effect further. Furthermore, because the cell killing becomes statistically significant only at the highest pressure available to us we were unable to compare cell killing vs. stress and stress rate to determine if stress rate is the relevant parameter for RPE cells, as was the case for EMT-6 cells. However, the lower cell killing observed for 20 ns risetime pulses compared to 10 ns risetime pulses at the highest stress used is consistent with stress rate being the significant parameter.

The lowest survival rate for transformed RPE cells exposed to stress waves was 50%. Figure 6 shows cell survival vs. number of pulses at the maximum obtainable stress (740 bars); increasing the number of pulses from 20 to 150 did not, within the experimental error, increase cell killing.

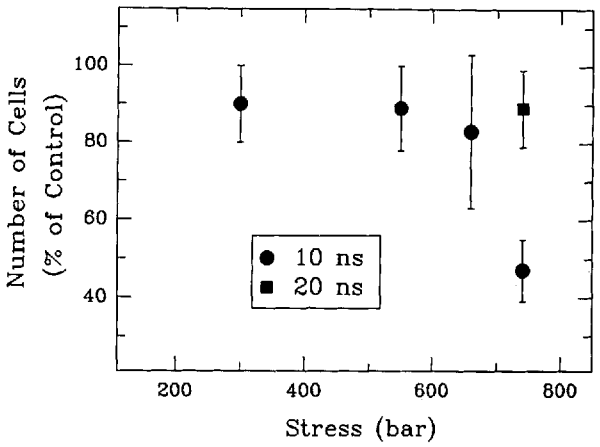

Fig. 5. Number of surviving cells, expressed as percent of unirradiated control cells, vs. pressure for immortalized RPE cells subjected to 20 pulses and analyzed 4 hours after irradiation. Both ArF and KrF laser pulses, which produced stress waves with rise times of 10 and 20 ns respectively, were used.

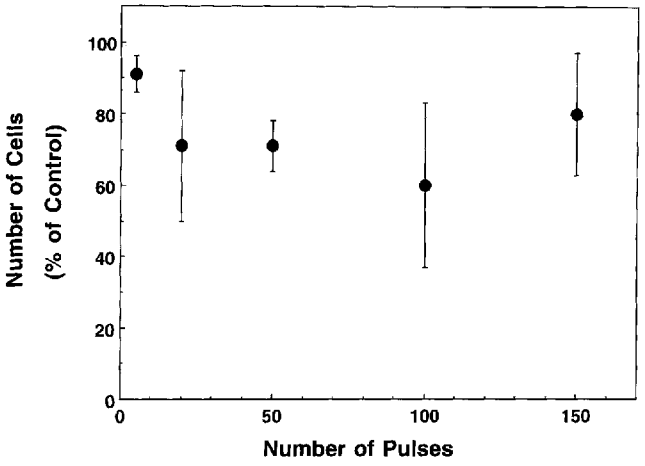

Fig. 6. Number of surviving cells, expressed as percent of unirradiated control cells, vs. number of pulses for immortalized RPE cells subjected to 740 bars stress and analyzed 4 hours after irradiation. ArF laser pulses were used.

In contrast to the behavior of the transformed cell line, experiments using normal RPE cells did not show any cell killing for up to 150 pulses at the maximum stress we could generate (740 bars).

Transmission electron microscopy of the normal RPE cell line confirmed the presence of melanosomes in the cytoplasm. No basal differentiation such as basal infolding was noted. In contrast, the immortalized cell line showed no melanosomes. The remainder of the cytoplasmic organelles showed similar distributions and quantities. Cells exposed to stress transients showed morphological alterations; however, no changes were identified that were specific for stress-induced damage. Near threshold these would include characteristic swelling of the mitochondria and the endoplasmic reticulum. More severe, above threshold, damage would show peripheral condensation of the nuclear chromatin, disruption of the mitochrondria and endoplasmic reticulum, swelling of lysosomes and disruption of cytoplasmic filaments [17]. The normal RPE cell line exposed to the laser-induced stress transients and the control cells showed no differences in any of these measures of mechanical injury by electron microscopy. The transformed RPE cells showed a mixture of cells with either no changes or damage and damaged cells showing the changes described above. Figure 7 shows representative electron micrographs of both normal and transformed RPE cells following exposure to stress transients as well as electron micrographs of unirradiated cells from control experiments.

DISCUSSION

The present experiments show a number of effects not observed in our earlier work demonstrating that damage to EMT cells is dependent on stress wave rise time rather than peak amplitude alone. In contrast to the behavior of the EMT-6 cells, the cell survival vs. peak stress curve shows a threshold-like behavior, with cell killing increasing sharply at the higher pressures. Since substantial cell killing occurs only at the highest stress, there is insufficient data to determine if mechanical damage to RPE cells depends on peak stress or stress wave rise time. Second, cell killing saturates with increasing numbers of pulses; regardless of the number of pulses applied we have not been able to destroy all the cells. Finally, the normal and transformed cell lines show different susceptibility to stress transients, with no cell killing obtained for the normal cell line.

The difference between the response of EMT-6 and RPE cells raises the question of whether the internal structure of cells may affect the response to stress wave. There are a number of differences between the two cell lines. The EMT-6 cell line is an immortalized mouse breast sarcoma cell which contains vimentin intermediate filaments while RPE cells have a predominance of keratin intermediate filaments. The EMT-6 cells have a spindle cell morphology while the RPE cells are more polygonal. RPE cells have

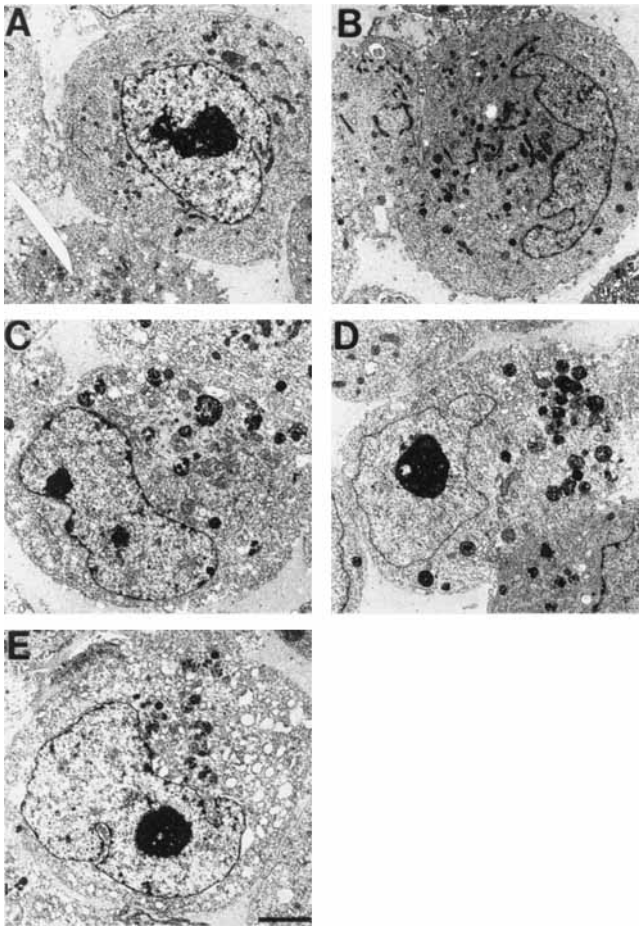

Fig. 7. **a:** Transmission electron micrograph of normal RPE cell from a control experiment in which there was no exposure to stress transients. **b:** Transmission electron micrograph of normal RPE cell following exposure to stress transients of 600 bars. Note the similar appearing mitochondria, nucleus, and lysosomes. **c:** Transmission electron micrograph of transformed RPE cell from a control experiment. **d:** Transmission electron micrograph of transformed RPE cell following exposure to stress transients of 600 bars. This cell is representative of those cells showing no damage. **e:** Transmission electron micrograph of transformed RPE cell following exposure to stress transients of 600 bars. Damage is demonstrated by swollen mitochondria and endoplasmic reticulum. (Bar = 3 μm.)

desmosomal attachments while EMT-6 cells do not. The importance of these differences will require further experiments to assess.

The present experiments demonstrate only incomplete killing of transformed RPE cells using the range of stress transients available to us. The fact that the surviving cells continue to grow suggests that normal cell growth can be a significant mechanism for reversing stress wave damage limited to the cellular level. It is worth noting, however, that in our experiments the cells are imbedded in a gel which consists only of collagen and buffer. In the in vivo situation or possibly even in RPE preparations the cellular environment may contain components whose entry into the cell could be toxic. The transmission electron microscopy indicates that there are not gross structural alterations that persist after exposure to the stress transients and does not identify structural elements that are associated with cell survival or death, a finding similar to our previous experiments in other systems.

The apparent saturation of the cell killing effect is consistent with the presence of a subpopulation of cells with different mechanical properties. The variation of mechanical properties could be related to a distribution of cell sizes or to a possible dependence on cell cycle. The latter hypothesis is supported by the observation that cells grown to full confluence could not be damaged by stress waves and by the fact that the doubling time in the sensitive transformed cell line was shorter than that in the normal cells. The high rate of cell survival observed in these experiments indicates that lysosomes were not disrupted. The lysosomes in these proliferating cells may be too small (~1 μm) to be affected by the 15 μm spatial gradient achieved here and therefore, do not release their enzymes. It would be interesting to know if expansion of the lysosomes, by lipofuscin for example, would alter the sensitivity of the cells to these stress waves. Finally, the possibility that the viral transformation of cells might have caused some unknown, but important alteration in membrane proteins can not be disregarded.

The mechanisms of cell killing by stress waves remain to be established; one possible mechanism involves transient opening of the cell membrane. Time-resolved fluorescence imaging of the transport of fluorescent marker dyes into cells subjected to shock waves indicates such a transient opening [25], as does the ability to deliver photosensitizing dyes and other molecules into cells using shocks [1,24,33]. While these experiments have established that transport of molecules across the cell membrane can be facilitated by shock waves they leave open the question of what, if anything, is transported across the cell membrane in these experiments. The fact that numerous experiments using both laser and lithotripter generated shock waves demonstrate cell permeabilization for variety of cell lines suggests that this is a general effect. On the other

hand cell killing by shock waves does not appear to be as general an effect. The differences in stress-induced cell killing between the two RPE cell lines studied here as well as the observed cell killing threshold, which is not found in EMT-6 cells, suggest that cell killing may involve other effects in addition to cell permeabilization. Further experiments will be needed to clarify this point.

The ability of mechanical effects accompanying optical breakdown to cause cellular damage in the eye has been previously demonstrated in experiments in which stress waves, cavitation bubbles and jets related to the interaction of cavitation bubbles with boundaries are all present. The present experiments have studied RPE cell damage in a better characterized and more controlled system and have demonstrated a number of cell specific damage effects which require further investigation. In future experiments, we plan to use higher power lasers and different stress generation techniques to extend the range of peak stress and stress rise time available to use in order to better understand the effects we have observed. In particular, we plan to determine if the difference between the normal and transformed cell behavior reflects only a difference in the threshold pressure for the onset of cell damage or is maintained over a larger pressure range.

ACKNOWLEDGMENTS

Supported in part by the Air Force Office of Scientific Research under a Brooks Air Force Base program on Ultrashort Laser Pulse Effects in Ocular and Related Media and NEI RO1-8121 (CKD).

REFERENCES

1. Flotte TJ, Anderson T, McAuliffe DJ, Hasan T, Doukas AG. Laser-induced enhancement of cytotoxicity: A new approach to cancer therapy. Proc SPIE 1993; 1882:122–129.
2. Cleary SF. Laser pulses and the generation of acoustic transients in biological material. In: Wolbarst M, ed. "Laser Applications in Medicine and Biology." Vol. 3, New York Plenum Press, 1977, pp 175–219.
3. Marshall J. Thermal and mechanical mechanisms in laser damage to the retina. Invest Ophthalmol 1970; 9:97–115.
4. Hofmann R, Hartung R. Laser lithotripsy of ureteral calculi. [Review]. Urol Res 1990; 18 Suppl 1:S49–55.
5. Delius M, Ueberle F, Gambihler S. Destruction of gallstones and model stones by extracorporeal shock waves. Ultrasound Med Biol 1994; 20:251–258.
6. Coleman AJ, Whitlock M, Leighton T, Saunders JE. The spatial distribution of cavitation induced acoustic emission, sonoluminescence and cell lysis in the field of a shock wave lithotripter. Phys Med Biol 1993; 38:1545–1560.
7. Coleman AJ, Saunders JE. A review of the physical properties and biological effects of the high amplitude acoustic fields used in extracorporeal lithotripsy. Ultrasonics 1993; 31:75–89.
8. Kaoutzanis MC, Peterson JW, Anderson RR, McAuliffe DJ, Sibilia RF, Zervas NT. Basic mechanism of in vitro pulsed-dye laser-induced vasodilation. J Neurosurg 1995; 82:256–261.
9. Zelman J. Photophaco fragmentation. J Cataract Refract Surg 1987; 13:287–289.
10. Zysset B, Fujimoto JG, Puliafito CA, Birngruber R, Deutsch TF. Picosecond optical breakdown: Tissue effects and reduction of collateral damage. Lasers Surg Med 1989; 9:193–204.
11. van Leeuwen TG, van Erven L, Meertens JH, Motamedi M, Post MJ, Borst C. Origin of arterial wall dissections induced by pulsed excimer and mid-infrared laser ablation in the pig [see comments]. J Am Coll Cardiol 1992; 19:1610–1618.
12. Zysset B, Fujimoto JG, Deutsch TF. Time-resolved measurements of picosecond optical breakdown. Appl Phys 1989; B48:139–147.
13. Fujimoto JG, Lin WZ, Ippen EP, Puliafito CA, Steinert RF. Time-resolved studies of Nd:YAG laser-induced breakdown. Plasma formation, acoustic wave generation, and cavitation. Invest Ophthalmol Vis Sci 1985;26:1771–1777.
14. Doukas AG, Zweig AD, Frisoli JK, Birngruber R, Deutsch TF. Non-invasive determination of shock wave pressure generated by optical breakdown. Appl Phys 1989; B53:237–245.
15. Vogel A, Busch S, Jungnickel K, Birngruber R. Mechanisms of intraocular photodisruption with picosecond and nanosecond laser pulses. Lasers Surg Med 1994; 15:32–43.
16. Doukas AG, McAuliffe DJ, Flotte TJ. Biological effects of laser-induced shock waves: Structural and functional cell damage in vitro. Ultrasound Med Biol 1993; 19:137–146.
17. Watanabe S, Flotte TJ, McAuliffe DJ, Jacques SL. Putative photoacoustic damage in skin induced by pulsed ArF excimer laser. J Invest Dermatol 1988; 90:761–766.
18. Zweig AD, Venugopalan V, Deutsch TF. Stress generated in polyimide by excimer laser radiation. J Appl Phys 1993; 74:4181–4188.
19. Yashima Y, McAuliffe DJ, Jacques SL, Flotte TJ. Laser-induced photoacoustic injury of skin: Effect of inertial confinement. Lasers Surg Med 1991; 11:62–68.
20. Doukas AG, McAuliffe DJ, Lee S, Venugopalan V, Flotte TJ. Physical factors involved in stress-wave-induced injury. Ultrasound Med Biol 1995; 21:961–967.
21. Kaver I, Koontz WW, Jr., Wilson JD, Guice JM, Smith MJ. Effects of lithotripter-generated high energy shock waves of mammalian cells in vitro. J Urol 1992; 147:215–219.
22. Smith FL, Carper SW, Hall JS, Gilligan BJ, Madsen EL, Storm FK. Cellular effects of piezoelectric versus electrohydraulic high energy shock waves. J Urol 1992; 147: 486–490.
23. Gambihler S, Delius M, Ellwart JW. Permeabilization of

the plasma membrane of L1210 mouse leukemia cells using lithotripter shock waves. J Membr Biol 1994; 141: 267–275.
24. Gambihler S, Delius M. Transient increase in membrane permeability of L1210 cells upon exposure to lithotripter shock waves in vitro. Naturwissenschaften 1992; 79:328–329.
25. Lee S, Doukas AG, Flotte TJ. Changes in membrane permeability from laser-induced stress transients. Conference on Lasers and Electro-optics 1995; 15:419(abstract).
26. Weiss N, Delius M, Gambihler S, Eichholtz-Wirth H, Dirschedl P, Brendel W. Effect of shock waves and cisplatin on cisplatin-sensitive and -resistant rodent tumors in vivo. Int J Cancer 1994; 58:693–699.
27. Gambihler S, Delius M. In vitro interaction of lithotripter shock waves and cytotoxic drugs. Br J Cancer 1992; 66: 69–73.
28. Rahman M. In vitro effects of high energy shock wave alone and combined with anticancer drugs on human bladder cancer cells. Urologia Internationalis 1994; 53: 12–17.
29. Prat F, Sibille A, Luccioni C, Pansu D, Chapelon JY, Beaumatin J, Ponchon T, Cathignol D. Increased chemocytotoxicity to colon cancer cells by shock wave-induced cavitation. Gastroenterology 1994; 106:937–944.
30. Vogel A, Lauterborn W. Acoustic transient generation by laser-induced cavitation bubbles near solid boundaries. J Acoust Soc Am 1988; 84:719–731.
31. Brummer F, Brenner J, Brauner T, Hulser DF. Effect of shock waves on suspended and immobilized L1210 cells. Ultrasound Med Biol 1989; 15:229–239.
32. Morgan TR, Laudone VP, Heston WD, Zeitz L, Fair WR. Free radical production by high energy shock waves—comparison with ionizing irradiation. J Urol 1988; 139: 186–189.
33. Holmes RP, Yeaman LD, Taylor RG, McCullough DL. Altered neutrophil permeability following shock wave exposure in vitro. J Urol 1992; 147:733–737.